DETC2019-97842

HYBRID FABRICATION OF A SOFT BENDING ACTUATOR WITH CASTING AND ADDITIVE MANUFACTURING

Marcos B. Oliveira
Expeditionary Robotics Lab
Mechanical & Industrial Engineering
Northeastern University
Boston, Massachusetts 02115
Email: oliveira.ma@husky.neu.edu

Alexander Lurie
Expeditionary Robotics Lab
Mechanical & Industrial Engineering
Northeastern University
Boston, Massachusetts 02115
Email: lurie.al@husky.neu.edu

David Ewen
Expeditionary Robotics Lab
Mechanical & Industrial Engineering
Northeastern University
Boston, Massachusetts 02115
Email: ewen.d@husky.neu.edu

Philip Long
RIVeR Lab
Electrical & Computer Engineering
Northeastern University
Boston, Massachusetts 02115
Email: p.long@northeastern.edu

Taskin Padir
RIVeR Lab
Electrical & Computer Engineering
Northeastern University
Boston, Massachusetts 02115
Email: t.padir@northeastern.edu

Samuel M. Felton[*]
Expeditionary Robotics Lab
Mechanical & Industrial Engineering
Northeastern University
Boston, Massachusetts 02115
Email: s.felton@northeastern.edu

ABSTRACT

In this paper, we present the design, modeling and, fabrication of a soft bending actuator that combines casting techniques and additive manufacturing. We performed tests to evaluate the bending actuator's angular deflection and tip force. We demonstrated flexibility in the process by varying the bladder material. We also showed the actuator's resilience to damage by cutting and puncturing the exoskeleton prior to operation. Finally, we integrated the bending actuator into a three-finger gripper configuration and performed a gripping test for four different objects with various weights and shapes. Results show that the curvature and force obtained in these actuators are comparable to other proposed bending actuators with a faster and more adaptable fabrication process. With these results we demonstrate that fast, effective, and versatile fabrication of soft robotic components can be attained by combining casting and additive manufacturing techniques.

---

[*]Address all correspondence to this author.

1 INTRODUCTION

Soft robotic grippers are a promising approach to manipulating delicate objects. [1]. While traditional robots include rigid components that can cause damage to people, the environment, or the objects that they handle [2], soft grippers prevent such damage due to their compliance. Each actuator, or "finger," is designed to be flexible, conforming around an object, allowing it to match complex contours and distribute gripping force [3].

One type of soft gripper technology is the fluid-driven soft actuator. A working fluid, usually air or water, is injected into an elastomer chamber and the material and geometry determine the direction and magnitude of actuation [4]. Soft pneumatic actuators (SPAs) have several benefits over traditional actuators including lower cost [5, 6], ease of assembly, delicate gripping [1], lower weight [7], safe human interaction [8], resilience to impact [9], and structural simplicity because they eliminate the need for motors, on-board control elements, and heavy structural links [10]. This is possible because elastic materials have the

FIGURE 1: A gripper composed of soft bending actuators using a hybrid fabrication method with casting and additive manufacturing

ability to simultaneously undertake functions related to structural stability and actuation. Therefore these components can reduce the complexity associated with their control in critical environments.

There are several types of SPAs. Pneumatic networks (PneuNets) use a bulky series of inflating chambers to expand axially or bend circularly [11, 12]. Other designs resemble radially expanding fingertips, applying pressure against a flat surface [13]. Fiber reinforced elastomer actuators have been tested and characterized. These use high-strength threads and an inextensible layer to dictate the direction of actuation [14, 15] which is induced by differential asymmetric straining of an elastomer bladder embedded with the inextensible and flexible layer (cloth or paper, for example) on one side and reinforced with a high strength thread wound around along its length.

A vast range of applications for pneumatic soft robots and actuators have been proposed. For instance, Soft Robotics Inc. (Cambridge, MA) commercializes pneumatically driven grippers generally used in industry for handling delicate and compliant elements such as processed food, fish, eggs, and glass bottles. Additionally, SPAs have been integrated in grippers [16] used for damage-free collection of samples in deep coral reefs thus leveraging the power of soft robotics in the field of marine biology.

For the fabrication of SPAs, several methods involving casting of silicone based materials have been proposed. These involve the design of molds into which material is poured for a final shape driven by cavities and features present in the mold. Despite the versatility that casting provides by offering the designer

a large set of material options, this process still presents some issues. Because of the complexity of some soft robotic systems, the design of molds and the fabrication process become complicated [17]. This increases the production time and the likelihood of errors during manufacturing. Also, because the bladder of SPAs tend to be fragile by the nature of the material which makes it extensible and soft, SPAs can be easily punctured or lacerated if handling sharp materials [18]. For many designs, any puncture renders the entire actuator beyond repair [4, 19, 20].

The idea for the fabrication process discussed in this paper was based on the limitations presented by the fabrication of fiber reinforced actuators proposed in [21, 22]. The fabrication method utilized for these actuators consists of a multi-step molding process combined with fiber reinforcement. Although effective, it is time consuming and difficult to automate. Furthermore, it requires the fabrication process be broken down into five main steps that occur in series: casting of the internal bladder, fiber winding around bladder and inextensible layer, casting of external skin layer, capping of one end of the actuator, and final capping of the opposite end of the bladder. This arrangement makes the entire fabrication process long and more susceptible to human errors given the number and complexity of steps. Also, in the event of severe bladder damage such as punctures or cuts, the entire actuator is discarded since the individual components are bonded together.

With the advent, broad commercialization, and technological evolution of 3D printers as well as the popularization of computer-aided design software, researchers and hobbyists have turned their attention to the use of additive manufacturing in the fabrication of soft robotic systems. This new approach allows the designer to prototype ideas more easily, accelerating the design phase and enabling fast and reliable integration of complex geometry into the design of soft robotic elements. However, despite ongoing research, limited selection of flexible resins and filaments for stereolithography (SLA) and fused deposition modeling (FDM) printers imposes a constraint on a broader use of 3D printing as a fabrication technique.

In this paper, we propose to combine the strengths of these two fabrication methods by 3D printing a flexible exoskeleton and integrating it with a cast polymer bladder. In so doing, we demonstrate a fabrication process that (1) is faster and easier than the fiber-reinforced fabrication process while achieving comparable performance, (2) can combine a wide variety of cast and 3D printed materials to optimize performance, (3) can be rapidly iterated by modifying the exoskeleton without building new molds for the bladder, and (4) results in improved damage resistance because the exoskeleton can be punctured or cut without piercing the bladder.

2 Fabrication

In order to avoid fiber-reinforcement and address the issues associated with it, we present a method for building soft actuators in which a 3D printed exoskeleton replaced the function of a strain-limiting layer and the high strength fiber. As depicted in Fig. 2c, a 3D printed mold set obtained from an SLA printer (Formlabs Form 2 SLA) was used in conjunction with a 12.7 mm aluminum half-round cylinder rod (McMaster #8242T41) and laser cut acrylic alignment pieces. First, the elastomer components were mixed (Fig. 2a) using an automated mixer (Thinky ARE-310) and then placed in a vacuum chamber (Fig. 2b) to remove air bubbles entrapped in the mixture. Then, the half-round cylinder was properly aligned and placed 5 mm from the end of the mold cavity using the mold cap geometry and laser cut acrylic alignment pieces (Fig. 2c). The mixed material was then poured into the mold (Fig. 2d) and left to cure (Fig. 2e). The elastomer material determined the cure time which can range from 2 hours to about 16 hours at room temperature of 25°C. Faster cure times can be as low as 20 minutes for some materials when placed in an industrial oven at 60°C. After curing was complete, the bladder was removed from the mold and the aluminum core extracted from the bladder using an air gun (Fig. 2f). The design of the bladder assumed the same cross sectional dimensions as shown in [23] with a bladder thickness of 3 mm. It is worth noting that the bladder thickness used in this paper was equivalent to the 2 mm thickness used in [23] which did not account for the external silicone layer fixing the fiber on the actuator.

In parallel with the casting process, an exoskeleton was 3D printed. It consisted of a 120 mm by 26 mm by 3 mm flexible base reinforced with nine equally spaced semi-circular arcs along its length. We varied the ring spacing to determine an effective gap width and observed that with fewer than nine arcs the bladder material started to plastically deform at low pressures whereas an increased number of arcs further constrained final bending angles. The first arc had a larger outer radius for later attachment of the soft actuator on a laser cut acrylic base plate for testing. Three holes radially placed around the opening of this arc allowed the soft actuator to be attached using M3 bolts and nuts. In order to make the exoskeleton, a Lulzbot Taz6 FDM printer equipped with a TAZ FlexyDually Tool Head v2 was used to print the structure. To achieve flexibility of this structure, we used NinjaFlex (NinjaTek). The software used to generate the
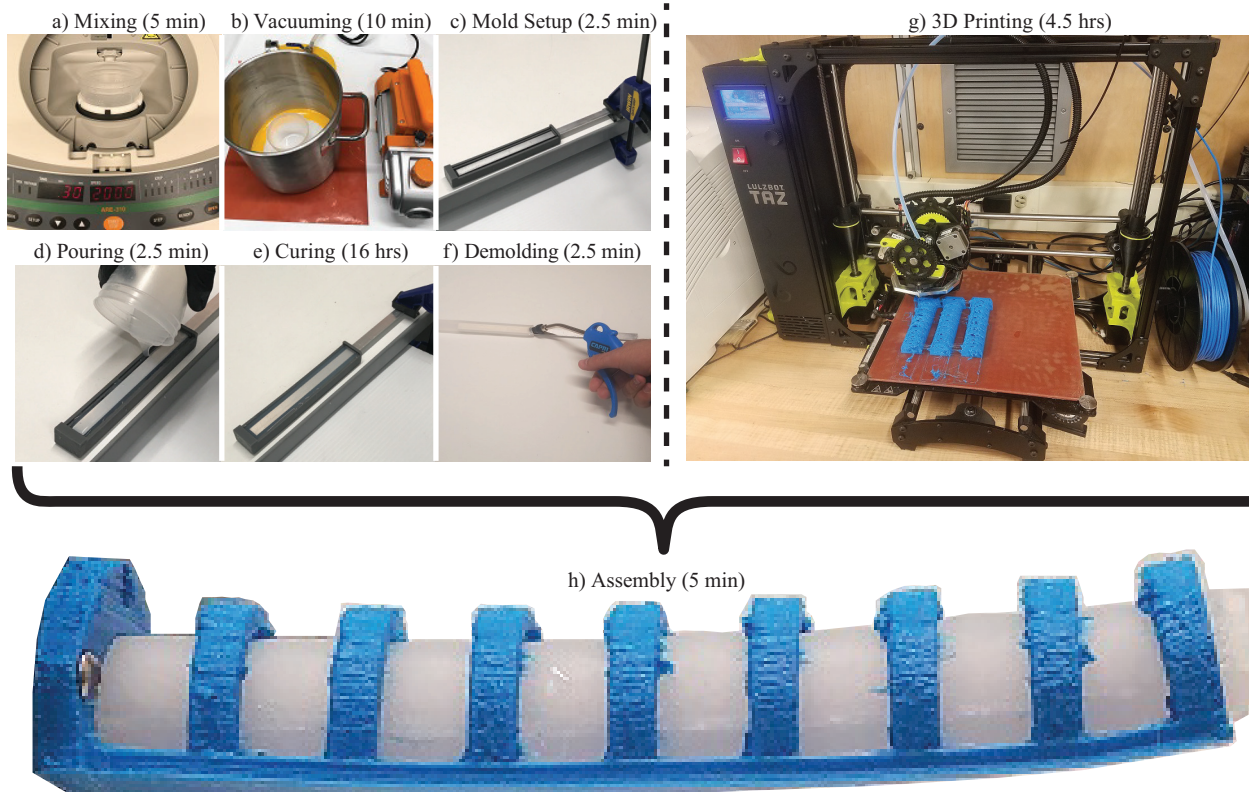
FIGURE 2: The hybrid fabrication method. a) Mixing elastomer components, b) vacuuming, c) setup of bladder mold components, d) pouring mixed material, e) curing, f) demolding bladder, g) 3D printing done in tandem with molding procedures, and f) final assembly of bladder and exoskeleton.

gcode for the print was Cura (Lulzbot). Total printing time of one soft exoskeleton including trimming of the external shell was approximately 4.5 hours.

After making both elements, the bladder was placed inside the exoskeleton. A quick-disconnect fitting with a barbed end (McMaster #5012K71) was inserted in the open end of the actuator. At this point, the exoskeleton was installed on a laser cut acrylic base and cable ties were used to seal the actuator around the fitting (Fig. 2h).

The 3D printed exoskeleton approach in conjunction with the technique of distal core alignment and tight sealing of fittings using cables ties simplified the five-step serial fabrication process of traditional fiber reinforced actuators to a double paralleled step process. Therefore this approach was expected to reduce the overall fabrication time by at least 50%.

Table 1 provides a comparison between fabrication times associated with four different bending actuator designs. Assuming same materials, techniques and equipment applied, we can conclude that our hybrid fabrication method was twice as fast as the manufacturing of fiber reinforced actuators. Additionally, it was comparable to the PneuNets design but significantly slower than exclusively 3D printed designs. Nonetheless, because of its faster maintenance and easier design iteration, our hybrid fabrication method for a bending actuator is an interesting alternative to PneuNets actuators. It also offers a larger selection of bladder materials which cannot be accomplished with exclusively 3D printed designs.

3 Mechanical Model

The soft bending actuator is modeled as a composite beam that bends due to the internal pressure induced within its hollow section according to Euler-Bernoulli beam theory. In order to characterize the relationship between the input pressure P and the output bending angle ψ, we developed a model that seeks the system's equilibrium by finding the minimum total potential energy associated with it.

The total potential energy of a conservative system Π_{sys} can be obtained by the difference between strain energy U_{sys} and work W_{ext} done by external loads. For the soft bending actuator, the total strain energy developed is due to the bending of the bladder ($U_{bending}^{bl}$) and, the exoskeleton ($U_{bending}^{sk}$) (Eqn.1).

$$U_{sys} = U_{bending}^{bl} + U_{bending}^{sk} \tag{1}$$

In order to simplify the analysis, we assumed a rectangular beam shape for the skeleton component. The cross section of the bladder was assumed to remain unchanged and the soft bending actuator's curvature $\frac{\psi}{L}$ was assumed to be uniform throughout

TABLE 1: Comparison between fabrication times for PneuNets, Fiber Reinforced, 3D Printed and Hybrid designs. Time (in parentheses next to each step, units are minutes) are based on authors' estimates using their own equipment and processes.

3D Printed	PneuNets	Fiber Reinforced	Hybrid	
3D Printing (270)	Mixing (5)	Mixing (5)	Mixing (5)	3D Printing (270)
	Vacuuming (10)	Vacuuming (10)	Vacuuming (10)	
	Pouring (2.5)	Pouring (2.5)	Mold Setup (2.5)	
	Initial Oven Cure (15)	Curing (960)	Pouring (2.5)	
	Base and top seaming (2.5)	Demolding (2.5)	Curing (960)	
	Curing (960)	Fiber threading (15)	Demolding (2.5)	
	Demolding (2.5)	Mixing (5)	Assembly (5)	
	Assembly (2.5)	Vacuuming (10)		
		Pouring (2.5)		
		Curing (960)		
		Demolding (2.5)		
		Assembly (2.5)		
TOTAL (min) 270	**1000**	**1977.5**	**987.5**	

its length. In order to find the system's equilibrium, we used a MATLAB script to inspect the total potential energy of the actuator for bending angles ψ ranging from 0° to 360°. To calculate the bending strain energy we use Eqn.2, where E is the material's Young's Modulus, I is the second moment of area and L is the component's length. It is noted however that the second moment of area I is calculated based on the bending neutral axis for a component.

$$U_{bending} = \frac{E\psi^2 I}{2L} \quad (2)$$

Usually, neutral axes cross the centroid of simple structures. However, in this case, the composite nature of the actuator and its stiffening upon pressurization required us to use a minimum energy approach. Its location is found through an iterative method where it is varied from the centroid of the skeleton to the centroid of the bladder. The position which minimizes the total potential energy of the system is then used.

Finally, the external work W_{ext} done is the product between the hydrostatic pressure (P), the solid internal cross sectional area of the bladder (A_B) and its change in total length ΔL (Eqn.3). This change in total length is caused on the bladder by the applied pressure P. It can be obtained by the difference between the actuator's stretched length and its initial length. The stretched length is calculated as the ratio between the bending angle ψ and the actuator's curvature which is a function of the neutral axis position. Therefore the equilibrium of the system is dependent upon the localization of the neutral axis position that balance the strain energy terms and the external work applied to it.

$$W_{ext} = P\,A_B\,\Delta L \quad (3)$$

Using Eqn.2 for the skeleton and the bladder individually and, Eqn.3, we calculate the total potential energy of the system given by (Eqn.4). By selecting the bending angle ψ and the neutral axis location that minimize the total potential energy of the system via an iterative method, we obtain the final equilibrium state for given material and pressure inputs.

$$\Pi_{sys} = U_{bending}^{bl} + U_{bending}^{sk} - W_{ext} \quad (4)$$

4 EXPERIMENTS
4.1 Bending Angle

In order to validate our experimental model for different materials, we performed bending angle tests with three different bladder materials. The materials tested were Dragon Skin 30 (Shore 30A by Smooth On), Dragon Skin 10NV (Shore 10A by
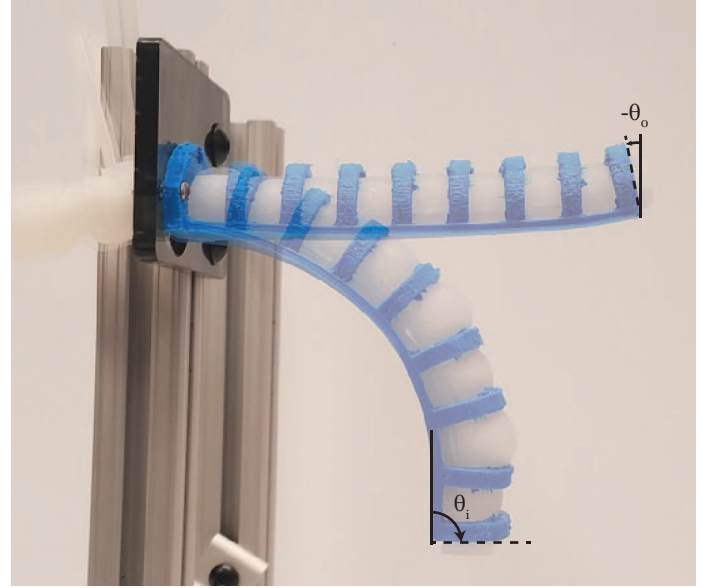
FIGURE 3: Bending angle test setup showing initial angle θ_o and bending angle obtained by pressurization θ_i. Bending angle ψ is defined as θ_i-θ_o.

Smooth On), and Elastosil (Shore 28A by Wacker Chemie) with Young's moduli of 1 MPa [24], 0.09 MPa [25] and, 0.262 MPa [26] respectively. We fabricated three bending actuators of each material which were tested for different pressure ranges depending on the material chosen and the maximum bending angle allowed by the test setup.

We mounted each soft finger on a test frame and the curvature of the actuator was photographed using an iPhone 7 camera mounted on a tripod. To track the bending angle observed at each one of the input pressures, we used a MATLAB script to quantify the actuator's bending. As depicted in Fig. 3, we took the difference of the final angle θ_i and the zero input pressure angle θ_o to calculate the final bending angle ψ.

We plotted data on bending angle ψ as a function of pressure (Fig. 4) to compare the results obtained against our model's predictions. Discrepancies observed between the model and the experimental data were in part due to the increase in cross sectional area of the pressurized finger and, the variation in material properties caused by errors in the mixing ratio of the silicone subcomponents. However, our mechanical model showed reasonable approximation to the test results indicating that local control of the bending angle ψ can be obtained through system's pressurization. In addition, we also observed that soft fingers made from Dragon Skin 10NV showed the largest angular displacements for lower pressures. However, they were not able to sustain larger pressures without plastically deforming. As expected, samples made from Dragon Skin 30 demonstrated the smallest amount of bending. These results show that a combination of exoskeleton

design and bladder material allows for different bending angles at different ranges of operating pressures. This concept can be used to tailor the design to meet different application requirements. Our actuators made from Elastosil showed an average bending angle of 296° for a maximum pressure of 165kPa. This is larger than the bending angle of approximately 180° at similar pressures obtained in [23] for a fiber reinforced actuator of the same cross sectional bladder dimensions. Therefore, we showed that our proposed design can achieve results comparable to other previous designs.

4.2 Blocked Force

To characterize the relationship of pressure versus the blocked force at the tip of our bending actuator, we performed a mechanical test on three samples with bladders made from Dragon Skin 30. We used a mechanical tester Mecmesin Multi-Test 2.5i coupled with a 10N load cell to measure the force at the tip of our bending actuator. Blocking at the tip was provided by a modified probe having a plate structure to block tip displacement. The center of the probe was placed at 115mm from the base plate where the bending actuator was mounted (Fig. 5). We pressurized the actuator at six different levels up to 193kPa with the aid of a manual pressure regulator (McMaster #6763K82). Further pressurization during this test was avoided since we observed that higher pressures caused material plastic deformation in the bladder component.

Results in Fig. 6 showed that the mean blocked force reached 2.6N at the maximum pressure. For comparison, in [21]
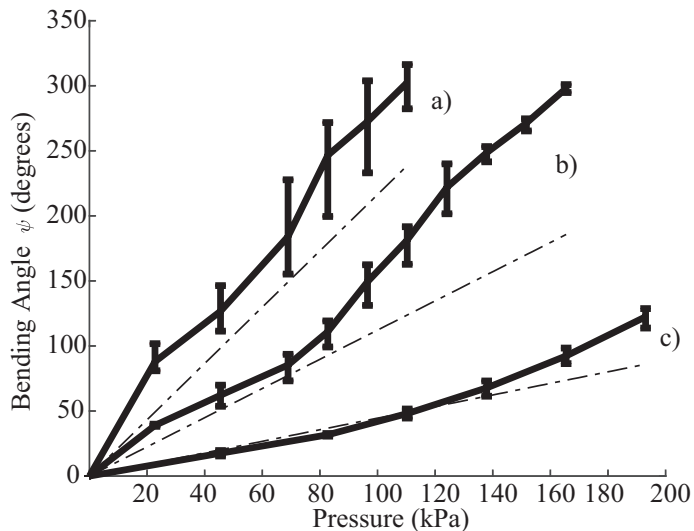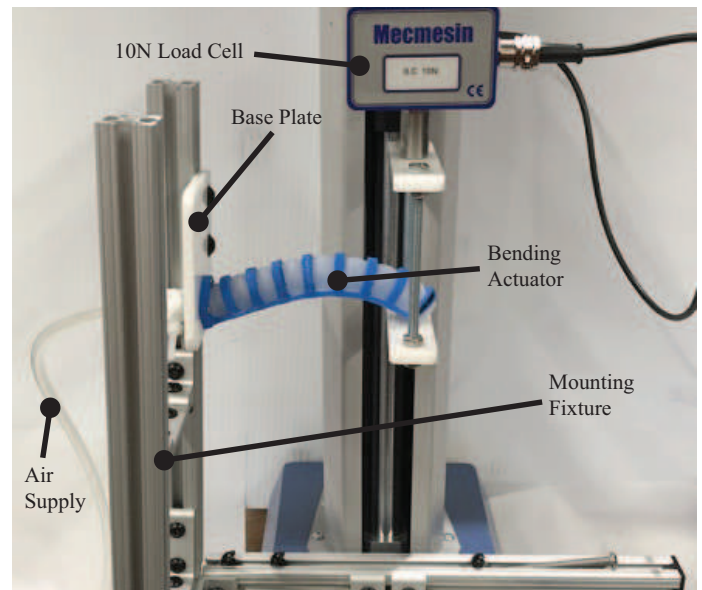
fiber reinforced actuators integrated with sleeves cut at different intervals showed a blocking force of approximately 2N indicating that our bending actuator was able to produce similar results as previous designs.
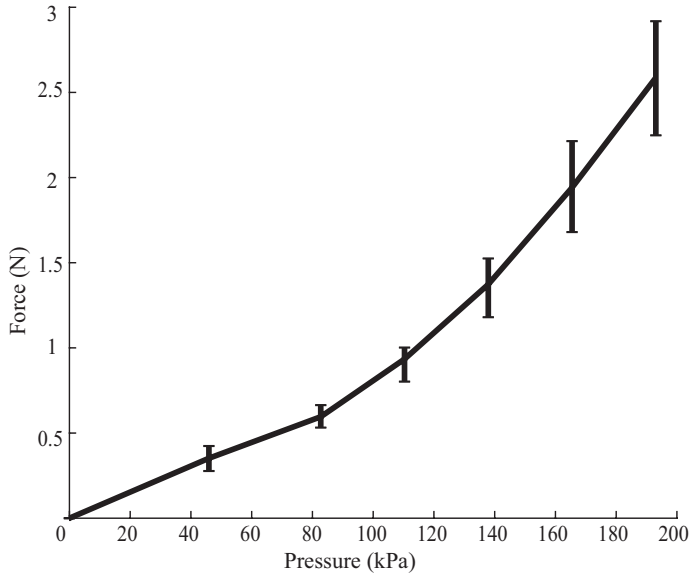
4.3 Damage Test

To demonstrate the resilience to damage of our bending actuator, we performed a damage test (video). We inflicted damage on the external side of the exoskeleton because we assumed that, being the part in contact with grasped materials, this is the side that is most exposed to damaging interactions. In this test, we used an X-Acto knife as a puncturing tool as well as a hacksaw, a metal scraper and a dremel cutting wheel as lacerating tools. In addition to damages induced on the base, we also used the dremel cutting wheel to make notches on the arcs of the exoskeleton.

As depicted in Fig. 7, the exoskeleton material, although being flexible, showed large resistance to damaging interactions. Out of the four tools used to induce damage, only the X-Acto knife and the dremel cutting wheel were able to draw visible damage on the exoskeleton. After each damaging interaction, we showed that the soft finger operated normally without any visible loss in performance. These results indicate that our bending actuator can operate even when damaged. This constitutes a great advantage over PneuNets, and fiber-reinforced designs which need to be discarded and fully replaced after being loaded under damaging conditions such as the ones demonstrated in this test.

FIGURE 4: Bending angle test results compared with model. Experimental data and model results shown in solid and dashed lines respectively. Error bars indicate standard deviation, N=3. a) Dragon Skin 10, b) Elastosil and, c) Dragon Skin 30

**FIGURE 5**: Blocked force test setup with mechanical tester and 10N load cell.

FIGURE 6: Blocked force test results for a soft finger made from Dragon Skin 30. Error bars indicate standard deviation, N=3.

4.4 Soft Gripper

In order to evaluate the applicability of our bending actuator, we integrated three of these soft fingers made with Dragon Skin 30 into a gripper configuration to test grasping and lifting of five different objects. The gripper was attached to a Sawyer (Rethink Robotics) robotic arm. The object to be grasped was placed on a table and the end-effector paths were programmed before each test. Objects of different shapes and weights were selected. Due to different shapes and rest positions of the objects, the end-effector orientation was adjusted to achieve successful grasp performance for each test.

As indicated in Fig. 8, all four objects were successfully grasped and lifted (video). These results demonstrated the effectiveness of our proposed bending actuator for grasping objects
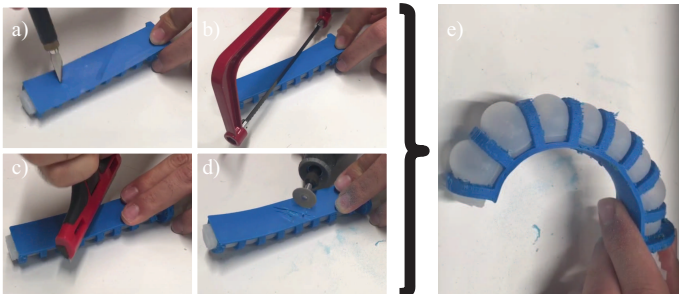
FIGURE 7: The soft finger under different damaging loads. a) X-Acto knife, b) hacksaw, c) metal scraper, d) dremel cutting wheel, and e) actuation after damaging loads

from a range of shapes and weights.

5 DISCUSSION

In this paper we proposed an alternative fabrication method for fiber reinforced actuators using an approach that combines molding and additive manufacturing techniques in tandem with each other. For traditional fiber reinforced actuators, the step of fiber winding dictated most of the complexity associated with the fabrication process in these actuators. By eliminating this step, we reduced the number of molding steps which can substantially reduce the time and complexity of the overall fabrication process of similar fiber reinforced soft bending actuators. In our hybrid approach, the exoskeleton eliminated the need for fiber reinforcement and replaced it with a parallel step involving additive manufacturing. Additionally, this method enabled material versatility associated with the cast internal bladder and a fast, reliable fabrication process used for the strain-limiting layers. This approach reduces the overall fabrication time of fiber reinforced actuators by approximately 50%, and is also an advantageous alternative to other bending actuator designs because of its faster maintenance, easier design iteration, and material versatility.

In addition, we presented a mechanical model that can be used to relate the pressure input to the final position of the soft bending actuator. We also showed that our proposed bending actuator presented similar angular displacements to other fiber reinforced actuators [23]. With regards to blocked force at the tip, we showed that comparable results can also be obtained using our design. Additionally, we showed that our design presents large resilience to damaging interactions and easy repair-ability without loss of performance because of its modular structure. Finally, we assembled a basic three-finger gripper using our actuator and a laser cut acrylic base. We attached this end-effector to the end of an industrial robotic arm to show successful grasping and lifting of objects of different shapes and weights.

Although the model was accurate for small deflections, its accuracy decreases at larger displacements. We believe that this deviation is due to the simplifying assumption that the bladder's cross section remains unchanged regardless of the pressure input. At high pressures, the bladder's cross sectional area gets larger due to its expansion on the segments where there is not a mechanical restriction provided by the skeleton arcs. Future work can address this issue by quantifying through image processing how much expansion is experienced at these sections of the bladder at given pressures. That will allow us to modify our model to account for this effect and improve our final results. We also want to develop an FEA model for this soft bending actuator where we can add frictional interactions that occur between the bladder and the exoskeleton during actuation. In doing so, we expect to obtain more accuracy, although at the expense of losing a parametric understanding of the system as whole.

One future avenue of research is adapting this design to other
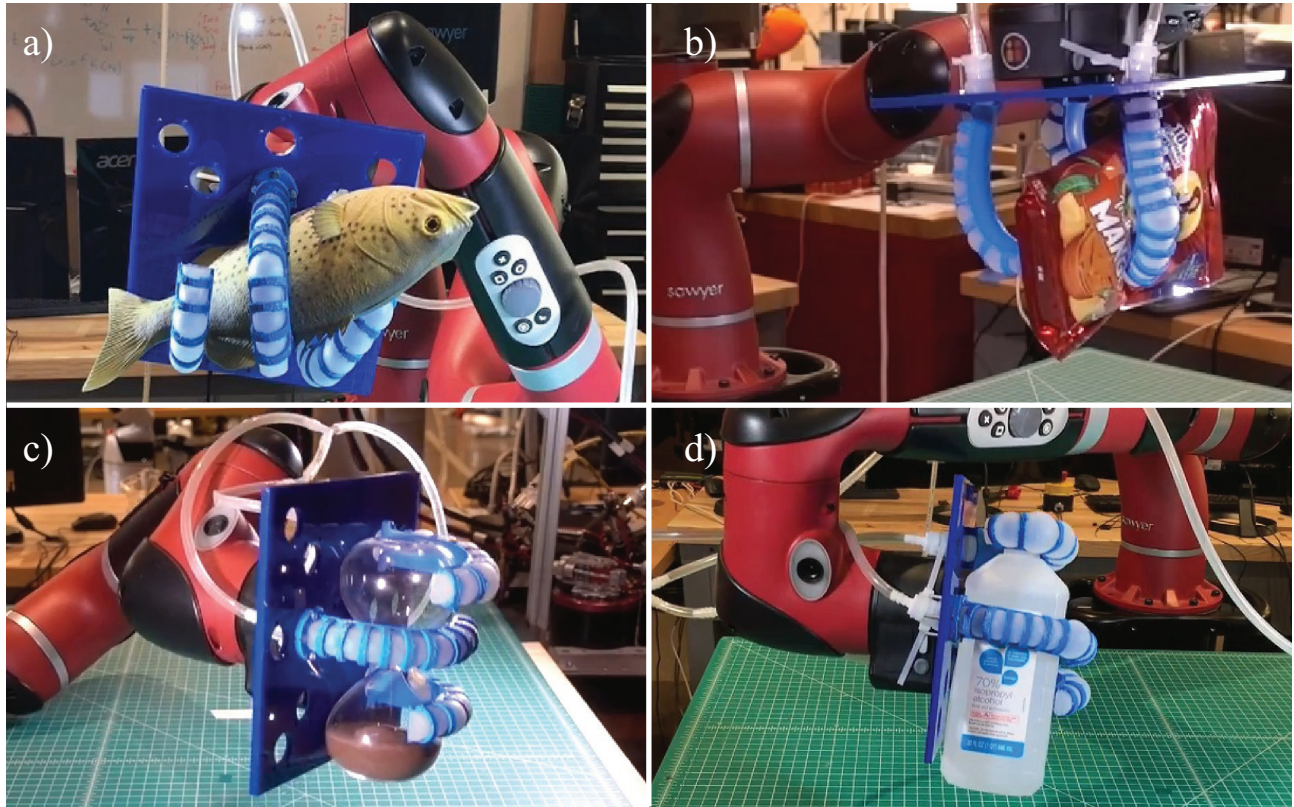
FIGURE 8: The soft gripper installed on a Sawyer robotic arm for grasping and lifting test. a) Fake fish (0.09kg), b) Candy package (0.17kg), c) Hourglass (0.25kg), and d) IPA bottle (0.90kg).

actuation modes such as twisting and expansion, similar to related research done in fiber reinforced actuators [15]. We believe that this will allow complex motions to be easily obtained in a faster and more reliable manner.

Finally, we want to integrate a control architecture for our soft gripper to enable automated operation, and testing under envisaged application scenarios. This combined with curvature sensing techniques will allow us to develop grippers that are capable of maneuvering objects as well as sensing their properties such as weight, texture and squishiness.

6 ACKNOWLEDGMENT

REFERENCES

[1] D. Rus and M. T. Tolley, "Design, fabrication and control of soft robots," *Nature*, vol. 521, no. 7553, p. 467, 2015.

[2] M. Cianchetti, T. Ranzani, G. Gerboni, T. Nanayakkara, K. Althoefer, P. Dasgupta, and A. Menciassi, "Soft robotics technologies to address shortcomings in today's minimally invasive surgery: the stiff-flop approach," *Soft robotics*, vol. 1, no. 2, pp. 122–131, 2014.

[3] D. Trivedi, C. D. Rahn, W. M. Kier, and I. D. Walker, "Soft robotics: Biological inspiration, state of the art, and future research," *Applied bionics and biomechanics*, vol. 5, no. 3, pp. 99–117, 2008.

[4] F. Ilievski, A. D. Mazzeo, R. F. Shepherd, X. Chen, and G. M. Whitesides, "Soft robotics for chemists," *Angewandte Chemie*, vol. 123, no. 8, pp. 1930–1935, 2011.

[5] R. F. Shepherd, F. Ilievski, W. Choi, S. A. Morin, A. A. Stokes, A. D. Mazzeo, X. Chen, M. Wang, and G. M. Whitesides, "Multigait soft robot," *Proceedings of the national academy of sciences*, vol. 108, no. 51, pp. 20 400–20 403, 2011.

[6] B. Trimmer, "Soft robots," *Current Biology*, vol. 23, no. 15, pp. R639–R641, 2013.

[7] C. Liu and S. M. Felton, "A self-folding robot arm for load-bearing operations," in *2017 IEEE/RSJ International Conference on Intelligent Robots and Systems (IROS)*. IEEE, 2017, pp. 1979–1986.

[8] C. Majidi, "Soft robotics: a perspective—current trends and prospects for the future," *Soft Robotics*, vol. 1, no. 1, pp. 5–11, 2014.

[9] R. V. Martinez, A. C. Glavan, C. Keplinger, A. I. Oyetibo, and G. M. Whitesides, "Soft actuators and robots that are resistant to mechanical damage," *Advanced Functional Materials*, vol. 24, no. 20, pp. 3003–3010, 2014.

[10] F. Iida and C. Laschi, "Soft robotics: challenges and perspectives," *Procedia Computer Science*, vol. 7, pp. 99–102, 2011.

[11] B. Mosadegh, P. Polygerinos, C. Keplinger, S. Wennstedt, R. F. Shepherd, U. Gupta, J. Shim, K. Bertoldi, C. J. Walsh, and G. M. Whitesides, "Pneumatic networks for soft robotics that actuate rapidly," *Advanced functional materials*, vol. 24, no. 15, pp. 2163–2170, 2014.

[12] P. Polygerinos, S. Lyne, Z. Wang, L. F. Nicolini, B. Mosadegh, G. M. Whitesides, and C. J. Walsh, "Towards a soft pneumatic glove for hand rehabilitation," in *2013 IEEE/RSJ International Conference on Intelligent Robots and Systems (IROS)*. IEEE, 2013, pp. 1512–1517.

[13] B. W. McInroe, C. L. Chen, K. Y. Goldberg, R. Bajcsy, and R. S. Fearing, "Towards a soft fingertip with integrated sensing and actuation," in *2018 IEEE/RSJ International Conference on Intelligent Robots and Systems (IROS)*, 2018.

[14] Y. Sun, Y. S. Song, and J. Paik, "Characterization of silicone rubber based soft pneumatic actuators," in *2013 IEEE/RSJ International Conference on Intelligent Robots and Systems (IROS)*. Ieee, 2013, pp. 4446–4453.

[15] O. Byrne, F. Coulter, M. Glynn, J. F. Jones, A. N. Annaidh, E. D. O'Cearbhaill, and D. P. Holland, "Additive manufacture of composite soft pneumatic actuators," *Soft robotics*, 2018.

[16] K. C. Galloway, K. P. Becker, B. Phillips, J. Kirby, S. Licht, D. Tchernov, R. J. Wood, and D. F. Gruber, "Soft robotic grippers for biological sampling on deep reefs," *Soft robotics*, vol. 3, no. 1, pp. 23–33, 2016.

[17] D. K. Patel, A. H. Sakhaei, M. Layani, B. Zhang, Q. Ge, and S. Magdassi, "Highly stretchable and uv curable elastomers for digital light processing based 3d printing," *Advanced Materials*, vol. 29, no. 15, p. 1606000, 2017.

[18] S. Kim, C. Laschi, and B. Trimmer, "Soft robotics: a bioinspired evolution in robotics," *Trends in biotechnology*, vol. 31, no. 5, pp. 287–294, 2013.

[19] E. T. Roche, R. Wohlfarth, J. T. Overvelde, N. V. Vasilyev, F. A. Pigula, D. J. Mooney, K. Bertoldi, and C. J. Walsh, "A bioinspired soft actuated material," *Advanced Materials*, vol. 26, no. 8, pp. 1200–1206, 2014.

[20] P. Maeder-York, T. Clites, E. Boggs, R. Neff, P. Polygerinos, D. Holland, L. Stirling, K. Galloway, C. Wee, and C. Walsh, "Biologically inspired soft robot for thumb rehabilitation," *Journal of Medical Devices*, vol. 8, no. 2, p. 020933, 2014.

[21] K. C. Galloway, P. Polygerinos, C. J. Walsh, and R. J. Wood, "Mechanically programmable bend radius for fiber-reinforced soft actuators," in *2013 16th International Conference on Advanced Robotics (ICAR)*. IEEE, 2013, pp. 1–6.

[22] P. Polygerinos, Z. Wang, K. C. Galloway, R. J. Wood, and C. J. Walsh, "Soft robotic glove for combined assistance and at-home rehabilitation," *Robotics and Autonomous Systems*, vol. 73, pp. 135–143, 2015.

[23] P. Polygerinos, Z. Wang, J. T. Overvelde, K. C. Galloway, R. J. Wood, K. Bertoldi, and C. J. Walsh, "Modeling of soft fiber-reinforced bending actuators," *IEEE Transactions on Robotics*, vol. 31, no. 3, pp. 778–789, 2015.

[24] M. Manti, T. Hassan, G. Passetti, N. d'Elia, M. Cianchetti, and C. Laschi, "An under-actuated and adaptable soft robotic gripper," in *Conference on Biomimetic and Biohybrid Systems*. Springer, 2015, pp. 64–74.

[25] H.-A. Oh, D. Park, K.-S. Han, and T. S. Oh, "Elastic modulus of locally stiffness-variant polydimethylsiloxane substrates for stretchable electronic packaging applications," *Journal of the Microelectronics and Packaging Society*, vol. 22, no. 4, pp. 91–98, 2015.

[26] G. Alici, T. Canty, R. Mutlu, W. Hu, and V. Sencadas, "Modeling and experimental evaluation of bending behavior of soft pneumatic actuators made of discrete actuation chambers," *Soft robotics*, vol. 5, no. 1, pp. 24–35, 2018.